

## Estimating of Crystallization Temperature of Mard-Abad (Karaj) Granitic Intrusion Using Mineralogy, Geochemistry and Morphology of Zircon Crystals

Z. Salehi<sup>1,\*</sup>, F. Masoudi<sup>2</sup>, M. Razavi<sup>1</sup>, N. S. Faramarzi<sup>3</sup>

<sup>1</sup> Department of Geology, Faculty of sciences, Islamic Azad University of Tehran shomal, Tehran, Islamic Republic of Iran

<sup>2</sup> Department of Geology, Faculty of sciences, Shahid Beheshti University, Tehran, Islamic Republic of Iran

<sup>3</sup> Department of Research and Development (R & D), Pars Kani Co. Tehran, Islamic Republic of Iran

Received: 9 June 2014 / Revised: 12 July 2014 / Accepted: 20 July 2014

### Abstract

Mard-abad calc-alkaline granite formed along the margin of active pull-apart or intra-continental plates, and it is post-collision granite type. Granophyric, perthitic and myrmekitic are main textures that could form from crystallization of hypersolvus source magma, which occurred under water vapor pressure of approximately 2 kb. During this study the temperature of formation of these granites has been estimated as high as 750 to 800 C° based on mineralogical and geochemical evidences. However, the thermometric measurement on zircon crystals has also been applied to achieve this goal. Zircon is of great importance because of its certain features such as resistance to chemical and mechanical processes, high melting point, and the ability of recording various geological events in its external structure as well as its internal texture. Crystallization of zircon is a function of temperature, chemical composition and the amount of water of the magma. The morphology of zircon crystals in Mard-abad granite points hybrid origin of granitic magma, which is in accordance with the geochemical evidence of the associated rocks. Such morphology also indicates to calc-alkaline and dry nature of the magma. The calculated crystallization temperature of these granite bodies is 700 to 800 C° based on morphology of zircons, 772.2 to 792 C° according to zircon saturation thermometry, and 760 to 800 C° based on the results from chemical analyses.

**Keywords:** Mard-abad granite; Geochemistry; Zircon morphology; Thermometry.

### Introduction

Mard-abad granitic intrusion is located within Central Iran zone and to the east of Kord-ha Mountain

(in the center of Karaj geological map). Based on stratigraphy, the age of the granite is considered to be younger than Eocene or Oligocene. There are rock units

\* Corresponding author: Tel:+98(21) 88663351; Fax: +98(21) 88663352; Email: msalehiz@yahoo.com

attributed to Late Eocene in contact of the granite. This granite body has been cut through by numerous dikes with NW-SE direction. Topographically, the intrusion appears as hilly landscape and form coarse rough reliefs. An aplitic phase in white color can be seen in some parts. Zircon mineral is among the minerals found in the granite. As a general fact, zircon with tetragonal crystallization system and as a secondary mineral can be widely seen within an extent ranging from crustal rocks to mantle xenolites, lunar rocks, meteorites, taktits, and specifically in felsic igneous rocks [1, 2]. The resistance of zircon to chemical and mechanical processes as well as its high melting point is so high that it can remain intact and unchanged within the earth crust for millions of years, and therefore it can survive from processes such as weathering, transportation, high temperature metamorphism and even partial melting. Moreover, the external shape and internal texture of zircon crystals depict the geological history experienced by these crystals. Belousova et al. [3], Corfu et al. [4] and Erdmann et al [5], demonstrated that the zoning in zircon crystals can be applied to understand magmatism, metamorphism and recrystallization processes. The zoning of magmatic zircons can be observed in polished sections with application of high resolution images such as BSE (Backscattered electron) and CL (Cathodoluminescence). Several researchers such as Pupin [6], Krasnobayev [7], Wang [8], Berezhnaya [8], and Wang & Kienast [10], have shown that there is a close relationship among the morphology of zircon, its origin, processes, chemical composition and geological setting of the source magma. For the first time, Pupin [6], categorized zircon crystals based on the relative growth of prismatic shapes of plane {100} as compared with plane {110}, and pyramidal shapes of plane {211} relative to plane {101}. According to their opinion, the relative growth of pyramidal shape is directly related with the chemical composition (the ratio of Al/ (Na+K)) whereas the relative growth of prismatic shapes is in direct relation with the crystallization temperature. Based on this categorization, zircons crystallized from peraluminous fluid would form pyramids whose plane {211} has been extensively developed as opposed to the zircons crystallized from Peralkalin fluid would form pyramids that their plane {101} has been developed. Water plays a significant role in zircon crystallization to such extent that zircons within water-saturated granites and pegmatites are identified by development of planes {101} and {110}. In magmas with low amounts of water content, zircons crystallize during a preliminary magmatic period whereas in magmas rich in water content, zircons start to crystallize right after the crystallization begins and continues with crystallization

of hydro-zircon rich in trace elements such as Y, U and Th [6, 4]. In this categorization the ratio of Al/ (Na+K) is presented as A index, and temperature of zircon crystallization as T index (Fig. 1).

Pupin [6], distinguished the three groups of granites by studying of the morphology of their zircon crystals (Fig. 2):

- 1- Zircons of high-temperature granites, which are associated with I-Type or mostly mantle-originated magmas (toleitic and alkaline types).
- 2- Zircons of medium-temperature hybrid granites

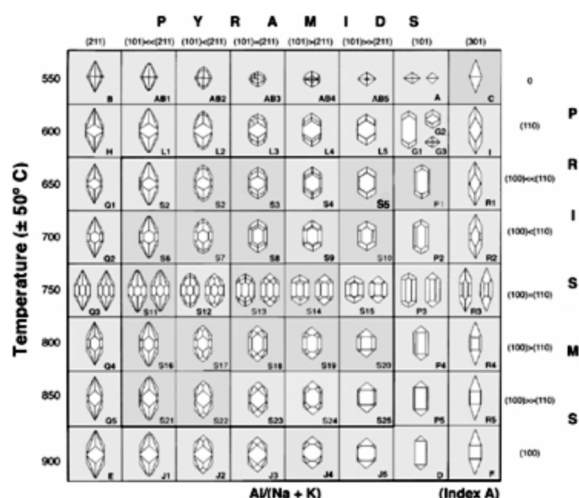


Figure 1. The location of various types of zircon crystals within petrogenetic categorization of Pupin (1982)

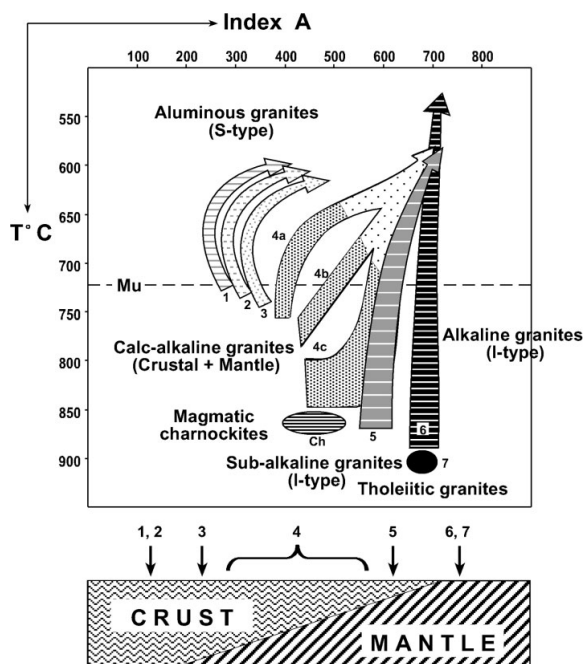


Figure 2. Determination of origin and magmatic series with use of morphology of zircon crystals, Pupin [6]

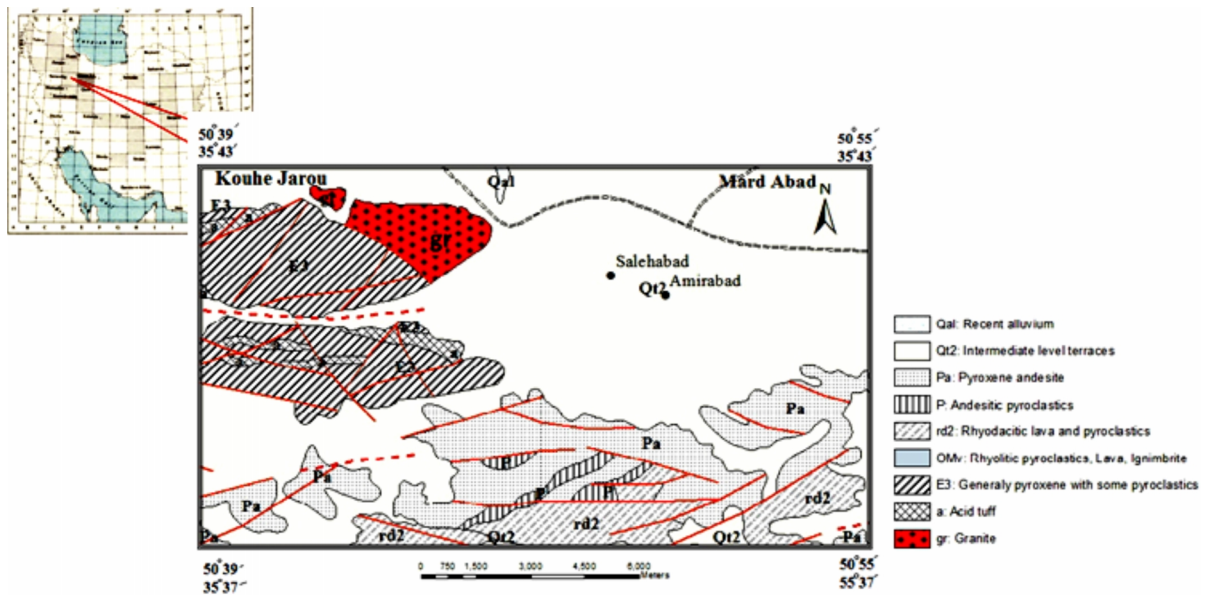


Figure 3. Location of the studied area and Mard-abad granite shown in Geological Map of Saveh with scale of 1:250,000

that belong to magmas with mantle and crust origins (granites of calc-alkaline series – alkaline and sub-alkaline).

3- Zircons of low-temperature granites that are related to S-Type magmas (derived from crust or aluminous granites).

According to Pupin [6], the temperature of magma is the most important factor in controlling the relative growth of prismatic shapes in zircon crystals. In addition to apply zircon shapes in identification of magma composition, these crystal shapes can be also used as thermometer.

## Materials and Methods

### 1. Geology of the studied area

Structurally Mard-abad granite is located in Central Iran, within Urumiyeh - Dokhtar zone, and geographically



Figure 4. Hilly landscape of Mard-abad granite

40 km to the southwest of Karaj city and 12 km to the southwest of Mahdasht in Alborz Province. The studied area is within 35° 37' and 35° 43' northern latitudes, and 50° 39' and 50° 55' eastern longitudes. It can be accessed via Tehran- Karaj- Mahdasht- Eshtehard- Boeinzahra road. The main road of Mahdasht to Akhtarabad-Saveh also runs through the south of the studied area (Fig. 3).

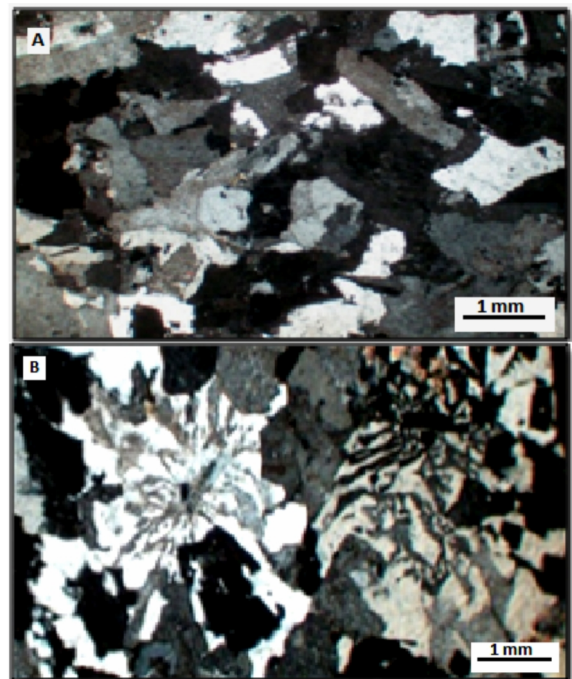


Figure 5. A) Granular texture B) Myrmekitic texture

**Table 1.** XRF and ICP-AES analyses on Mard-abad granite

No.	G-1	E1-90	E2-90	S-2	S-8
SiO <sub>2</sub>	71.82	69.73	71.00	67.93	71.08
Al <sub>2</sub> O <sub>3</sub>	12.15	12.77	13.57	13.60	12.02
Fe <sub>2</sub> O <sub>3</sub>	1.30	0.59	1.70	1.76	0.67
MgO	0.53	0.42	0.38	0.64	0.16
CaO	1.06	1.16	0.33	1.51	0.55
Na <sub>2</sub> O	7.21	3.43	3.74	3.43	2.92
K <sub>2</sub> O	2.29	5.88	5.56	5.31	6.04
TiO <sub>2</sub>	0.28	0.25	0.28	0.31	0.13
MnO	0.04	0.03	0.03	0.03	0.02
P <sub>2</sub> O <sub>5</sub>	0.06	0.04	0.06	0.09	0.02
Rb	149.40	162.70	198.70	163.80	179.80
Sr	193.94	123.50	41.67	209.93	105.02
Y	40.23	39.11	35.00	39.27	39.13
Cr	89.10	95.20	89.40	84.75	95.71
Zr	303.00	265.70	261.10	289.30	233.00
Nb	28.80	29.30	30.80	23.50	27.80
Ba	195.60	99.00	94.40	25.40	87.50
La	15.12	13.98	10.84	10.88	9.46
Ce	37.46	37.78	26.55	25.81	24.14
Nd	47.80	39.20	25.70	33.80	37.40
Sm	2.60	2.90	1.20	1.60	1.10
Tb	1.10	1.00	0.80	1.00	0.10
Yb	4.40	2.10	4.40	2.10	2.00
Hf	2.60	4.10	2.30	0.70	13.90
Ta	14.80	10.80	7.20	11.70	3.30
V	22.41	11.41	17.17	26.64	11.18
Pb	12.11	24.83	16.38	20.17	45.93
Cu	<5	40.65	41.21	<5	70.99
Co	6.20	4.94	5.71	7.40	5.03
Zn	45.65	80.00	43.23	27.81	72.48
Cs	12.40	15.20	13.80	21.00	14.10
Ga	18.60	21.60	21.00	20.60	23.40
Mo	5.00	10.33	8.11	4.66	22.49
Sn	11.10	13.60	4.60	18.40	7.20
Th	40.40	39.60	42.90	30.40	60.70
As	<10	<10	<10	<10	<10
Sb	<10	<10	<10	<10	<10
Dy	3.10	1.80	2.90	3.10	2.90
Ho	0.10	0.70	0.80	0.10	0.80
Er	0.30	0.73	0.43	0.33	0.43
Ag	<1	<1	<1	<1	<1
Be	2.47	2.41	2.12	2.37	3.15
Bi	<5	<5	<5	<5	<5
Cd	<1	<1	<1	<1	<1
Li	<5	<5	<5	<5	<5
Eu	1.30	1.50	1.50	1.50	1.50

## 2. Petrography of Mard-abad granitic intrusion

Topographically, the granite is seen in form of coarse rough reliefs (Fig. 4). In some areas around the granite body an aplitic phase in white color is detectable. Based on the classification of the rocks in the area, the studied granite can be grouped into four types of quartz-monzonite, monzo-granite, syeno-granite and alkali-feldspar granite. The textures

identified in various rocks in the area include perthitic, granophyric, granular and myrmekitic (Fig. 5). Granophyric and perthitic textures imply to emplacement of the granite body in shallow depth. Biotite, chlorite and iron oxides are more or less seen in all samples. In some samples, muscovites in form of veins or amorphous fillings can be found within the spaces between crystals. Light and dark fine-grained enclaves are observed inside the granite. These enclaves are andesite and tuff-andesite types and seen in the form of both angular and oval shapes, which were probably cut into pieces during the emplacement of the granite and placed inside the body. Notwithstanding the presence of these light and dark fine-grained enclaves, the origin of this granite is probably of mantle type. The dikes inside the body are of basic type with diabasic composition (doleritic), which occur parallel to each other in NW-SE direction. Compared south and east of the granitic body, the number of dikes penetrated into western part is more, with average thickness of 4 m. The number and thickness of the dikes decrease as moving southward and eastward that is probably due to the different effect of fluids on various parts of the body as it seems with increase in penetration of fluids the dikes grow more elongated and thicker.

Once microscopic studies carried out, five samples were selected, crushed and grinded at Iranian Mineral Processing Research Center (IMPRC), and analyzed using XRF method in the laboratory of Kharazmi University to measure their primary and secondary elements. Minor elements measured using ICP-AES method, these samples were analyzed in SSC lab in Russia using ELAN 9000 instrument, and the results are shown in Table 1.

## Results

The texture of Karaj Mard-abad granites includes

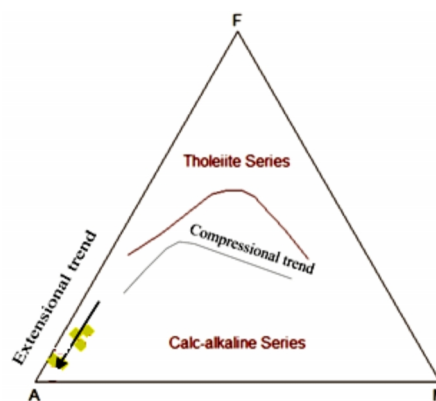


**Figure 6.** Diagram separating calc-alkaline series from tholeiitic series [11]; samples are situated within calc-alkaline

Estimating of Crystallization Temperature of Mard-Abad ...

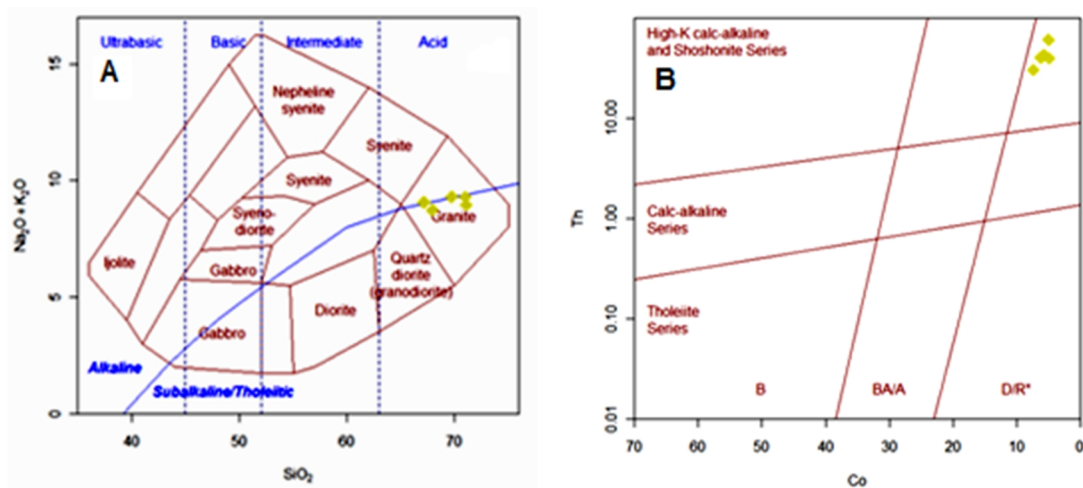


Figure 7. A)  $\text{Na}_2\text{O}+\text{K}_2\text{O}$  vs.  $\text{SiO}_2$  diagram [12]. Samples located along the border between calc-alkaline and sub-alkaline areas: B) Co vs. Th diagram [13]

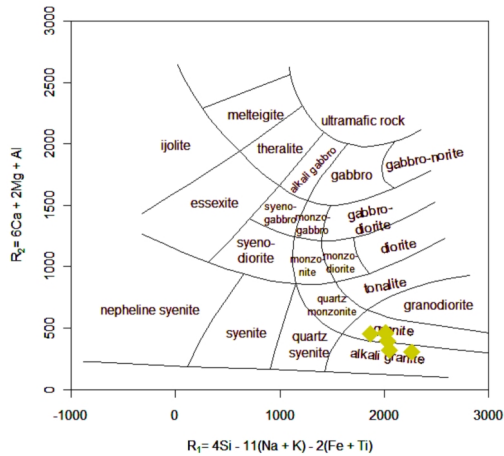


Figure 8. Analyzed samples plotted in De La Roche

granular, granophyric, myrmikite, and perthitic.

Mineralogically these granites contain quartz, alkali-feldspar, plagioclase, biotite, muscovite, clino-pyroxene (in some samples) and epidote. These granites fall within calc-alkaline area in AFM diagram [11] (Fig. 6), and situate within alkaline and sub-alkaline areas in TAS [12] and Hasti et al. [13] (Fig. 6 and 7). However, samples of granites are plotted within alkali-granite and granite areas in the diagram presented by De La Roche et al. [14] (Fig. 8) and Streckeisen and Le Maitre [15] (Fig. 9).

The nature of the granitic magma is magnesium and calc-alkaline to alkaline type [16], and with the exception of one sample that situates in peraluminous

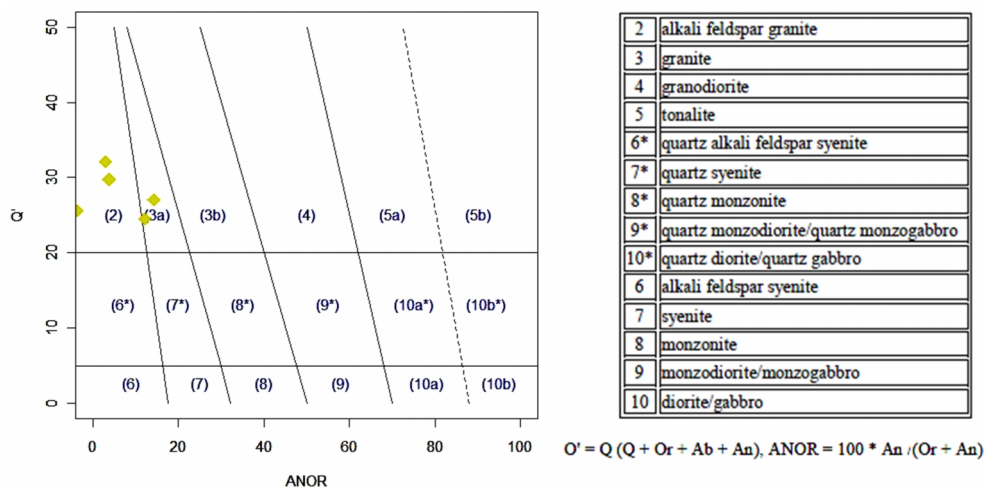


Figure 9. The position of studied samples in Streckeisen and Le Maitre [15], diagram

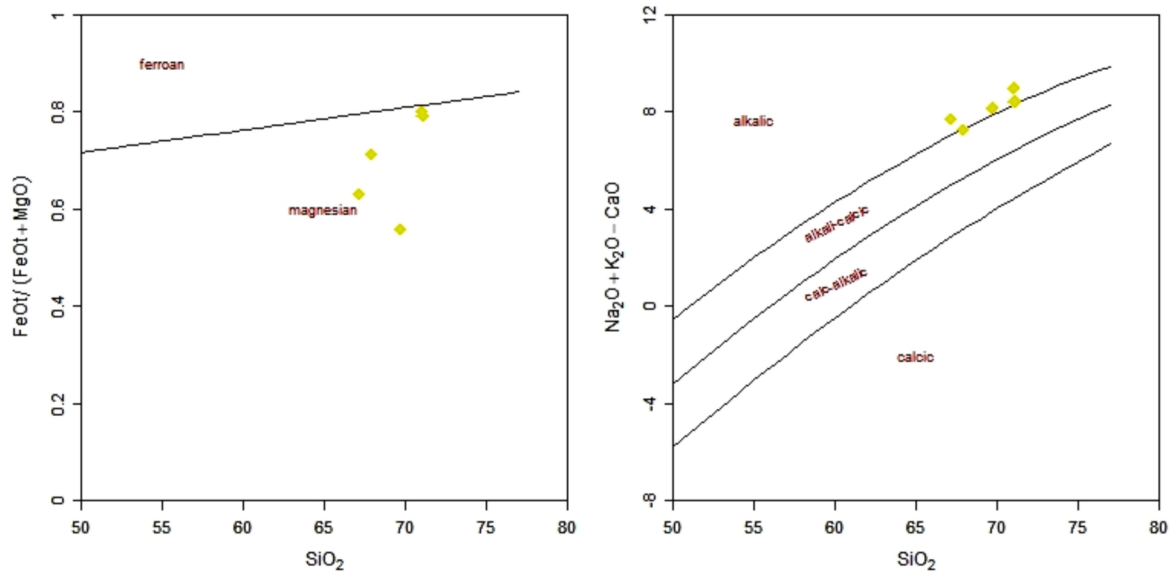


Figure 10. Determination of the nature of the studied granitic intrusion [16]

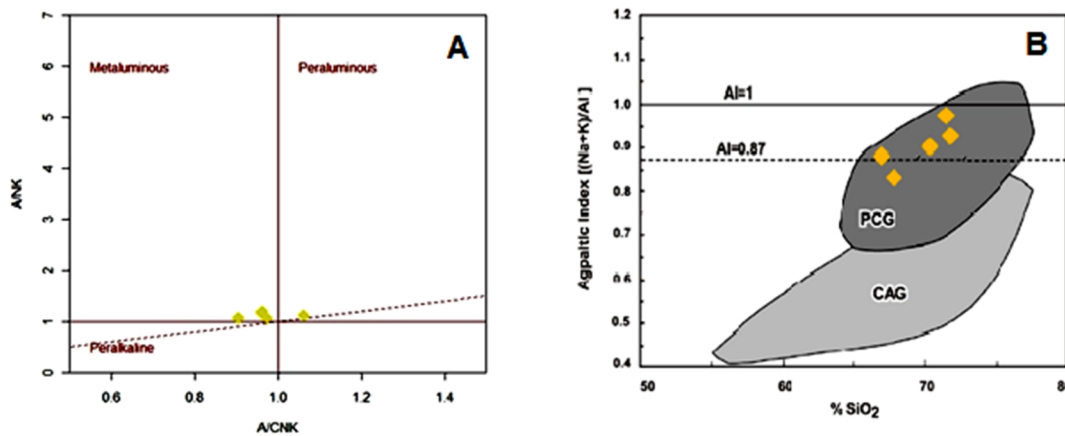


Figure 11. A) A/NK vs. A/CNK diagram [17]; B) Positive correlation between AI and SiO<sub>2</sub> is evidence for meta-aluminous nature of the granite [18]

area the samples often are on metaluminous area in A/NK vs. A/CNK diagram (molar OR mole ratio of Al<sub>2</sub>O<sub>3</sub>/(CaO+Na<sub>2</sub>O+K<sub>2</sub>O)) by Shand [17], (Fig. 11a). The positive correlation between AI and SiO<sub>2</sub> confirms the meta-aluminous nature of the granitic body in the studied area [18] (Fig. 11b).

Emplacement of granite was in within intra-plate area based on diagram of Harris et al. [19] (Fig. 12). Also, the proximity to AF line in AFM diagram indicates the formation of the granite along the margins of pull-apart plates or intra-plate (Fig. 6). It is confirmed by the emplacement of most samples within intra-plate area in tectonic settings separating diagram with use of

trace elements by Pearce et al. [20] (Fig. 13).

Eu/Eu\* vs. Ga/Al diagram (Fig. 14a), Wallen diagrams [21] (Fig. 14b, 14d) and Kleman & Twist diagram [22] (Fig. 14c) have been applied in order to study the origin of the granite intrusion in the studied area and also distinguish granite type. All samples are A-type.

In ternary diagrams separating granitoid types A1 and A2 based on Y-Nb-Zr/4, Y-Nb-Ce and Y-Nb-3Ga [23], all granite samples taken from the studied area are plotted inside area A2 and close to the border with area A1 (Fig. 15). It could imply that granites formed within a post-collision tensional setting behind the magmatic arc.

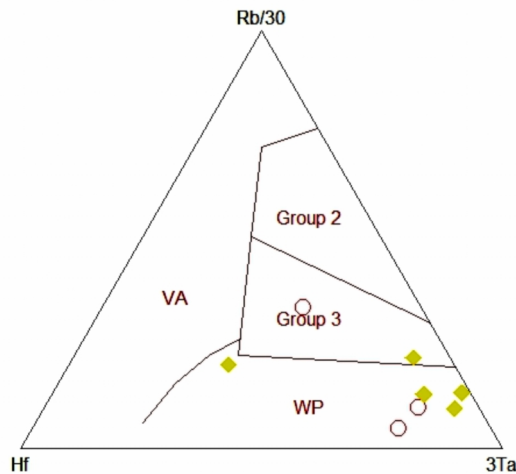


**Figure 12.** The position of granitic samples on Rb-Hf-Ta diagram separating tectonic settings [19]. In this diagram Group 2 is syn-collision granites, Group 3 represents granites formed in the final stage of collision to post-collision, VA shows volcanic arc granites, and WP contains intra-plate granites and most of the studied samples are in this area.

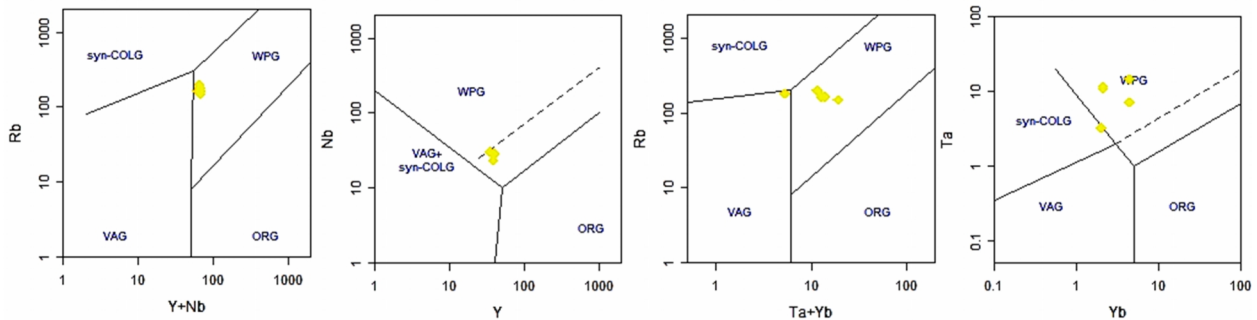


**Figure 13.** Trace elements separating tectonic settings diagrams [20]

## Discussion

### Approximate pressure and temperature of granitic magma

Studying texture and chemistry of granitic rocks could greatly help us realize temperature and pressure settings. Those granites emplaced close to the surface crystallize faster and under lower water pressure compared to those granites forms in deeper parts, and its effects the sort of solid liquid materializes within their alkaline feldspars (hypersolvus crystallization). If volatiles move out of the place, the magma follows dry liquidus and solidus curves, and cools down and crystallizes relatively fast. Under such circumstances crystals would not grow independently, and thus, simultaneous growth of quartz and feldspar crystals leads to creation of granophyric synchronous growth. However, if the water pressure stays high, liquidus and solidus curves drop to lower temperature and therefore potassic feldspar and sodic plagioclase crystals develop separately [24].

Considering the abundance of granophyric texture and presence of perthite in Mard-abad granite, it could be concluded that crystallization was hypersolvus type and occurred under water pressure of approximately 2 kilobars. Accepting this pressure and location of samples on Q – Ab – Or ternary diagram [25], the temperature at the time of creation of granitic magma is approximately calculated as high as 750 to 800 C° (Fig. 16).

### Temperature and chemistry of Mard-abad granitic magma using zircon crystals:

#### 1) Zircon crystals separation procedure

Two kilograms of suitable granitic sample crushed using jaw crusher machine in Geological Survey of Iran. A portion of samples with grain size of 100 to 200  $\mu$  selected using sieves. Once the samples washed and dried out, their iron-bearing minerals are picked out using magnet. With help of bromoform solution the

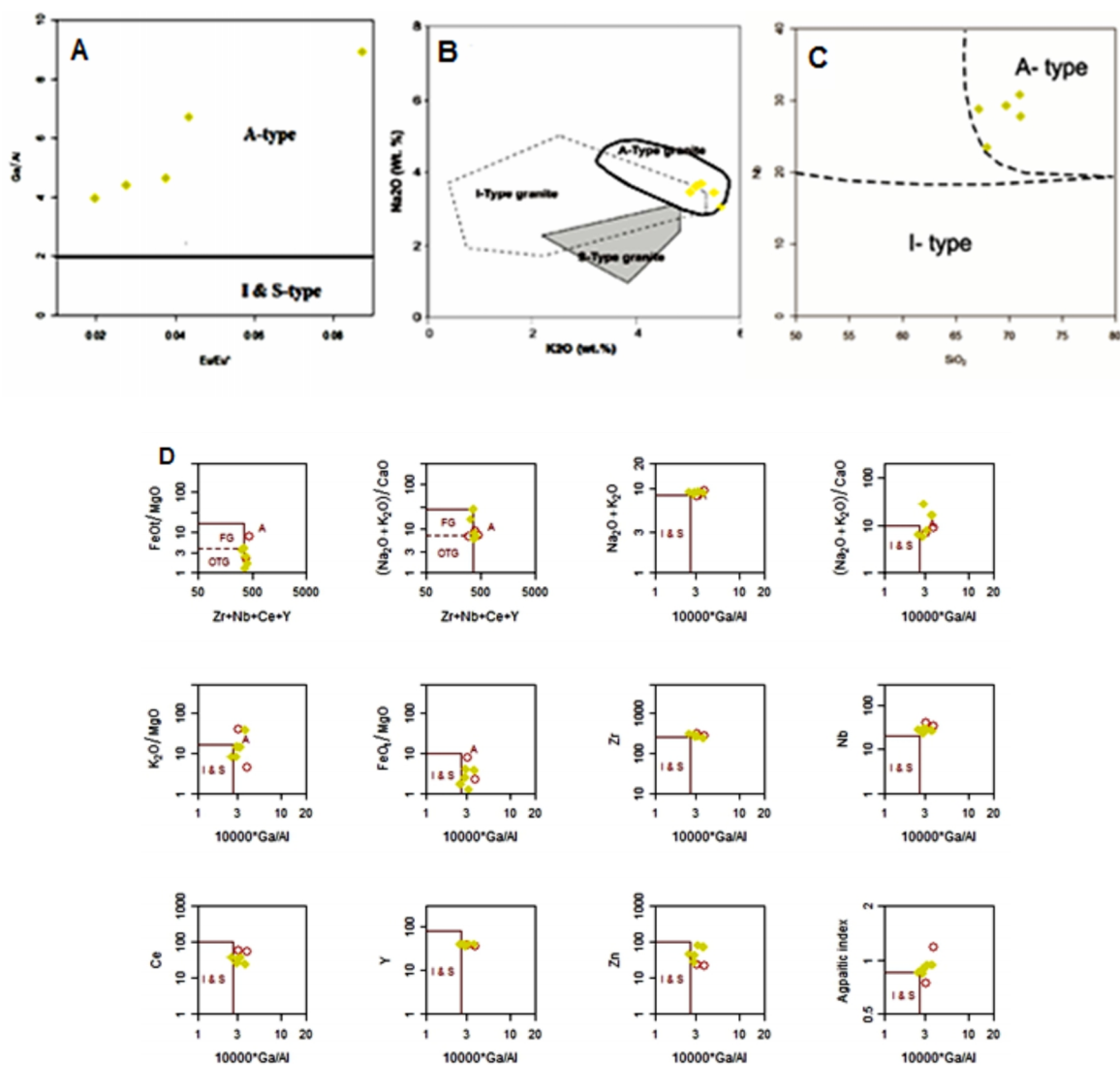


**Figure 14.** A)  $Eu/Eu^*$  vs.  $Ga/Al$  diagram for distinguishing granite types of S, I and P; B)  $Na_2O$  vs.  $K_2O$  binary diagram [21], in which all samples show A-type nature; C)  $Nb$  vs.  $Wt\%$  of  $SiO_2$  diagram to separate granite types of A and I [22]; D) Wallen diagrams [21], based on HFSE elements to separate granitoid types of A, I and S. All samples are A type.

heavy minerals are separated and then dried out in the oven. The next step was to separate zircon crystals from other heavy minerals and glued them onto slides using dual-component epoxy glue. To study the morphology of zircon crystals, a high magnifying electronic microscope is used to scan 40 selected zircon crystals with no evidence of roundness that are already glued onto the plate and covered with carbon. Then, I.A and I.T indexes (alkalinity index and thermal index) as well as length and width of these crystals are measured and their zoning studied.

## 2) Morphology of zircon crystals in Mard-abad granites

Regards to the morphology and shape of zircon crystals it's been observed that most zircon crystals are placed on S10, S14 and S18 areas of Pupin's zircon morphology classification, and to the lesser amount on S9, S13, S17 and S19 areas (Fig. 17). Honey yellow and red color zircon crystals do not show inclusions and zircons are sometime colorless. They are transparent to semi-transparent, and no hydro-zircon in form of synchronous growth is seen in them.

The average of I.A. index is 487.5 and 495.0 for I.T.

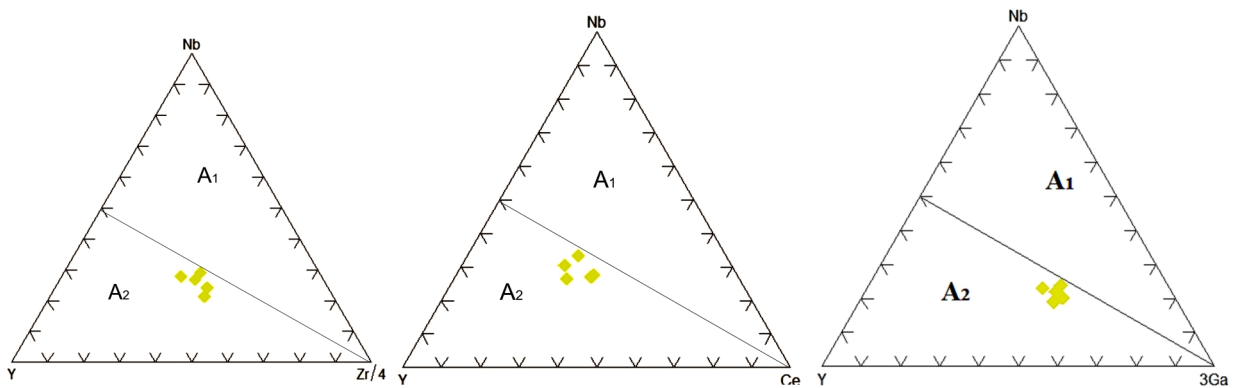


**Figure 15.** Ternary diagrams separating granitoid types A1 and A2 based on Y-Nb-Zr/4, Y-Nb-Ce and Y-Nb-3Ga [23], granite samples taken from the studied area are plotted inside area A2.

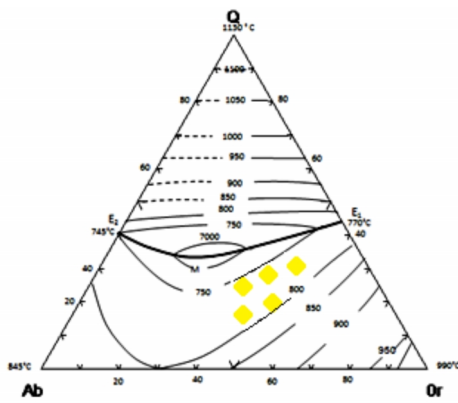


**Figure 16.** Q – Ab – Or ternary system at water pressure of 2 kb along with cotectic isomers [25]. The point M is the minimum value on cotectic line.

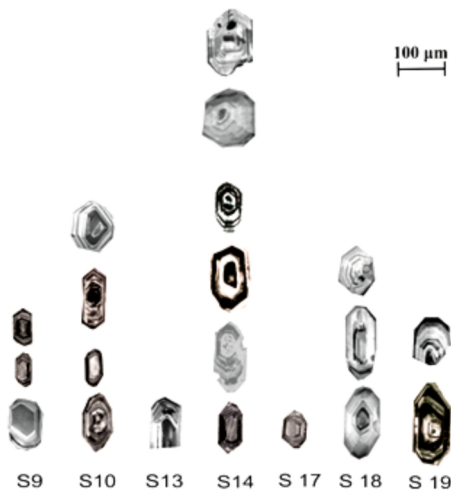


**Figure 17.** Zircon crystals of Mard-abad granite and their classification based on morphology after Pupin [6]

index. The value of Typological Evolutionary Trend (T.E.T) is to 40.56. In order to calculate T.E.T from the crossing point of I.A and I.T, a line with slope of ST/SA (standard deviation of index T/standard deviation of index A) is drawn. The value of this slope is equal to the Tangent of the angle between T.E.T axis and I.A axis. As seen in Fig. 17 the zircon crystals of the studied area fall in alkaline granite area. On the other hand, considering the morphological classification of zircons by Pupin [6], the shape of zircons imply their crystallization from a magma with hybrid origin (i.e. originated from both crust and mantle) at the temperature of 700 to 800°C (Fig. 18 and 19).

**Geo-thermometry with zircon crystals:**

**1- Geo-thermometry based on the shape of zircon crystals:**

Based on the morphology of zircon crystal, as previously seen in figures 17 and 18, the temperature of formation of zircons in Mard-abad granite is in the range of 700 to 800°C.

**2- Geo-thermometry based on zircon saturation:**

The concentration of zirconium in granites is often controlled by the degree of solubility of zircon in molten granite. If the composition of magma is consistent, the solubility of zircon is a function of temperature; however this concentration, to some extent, is dependent on the solvent composition [26]. Therefore the concentration of molten Zr and the composition of zircon minerals can be used as independent geo-thermometer in order to estimate the temperature of the magma. Janousek [27], believes the following parameters and conditions are required to apply this method:

- a. Metaluminous nature of magma

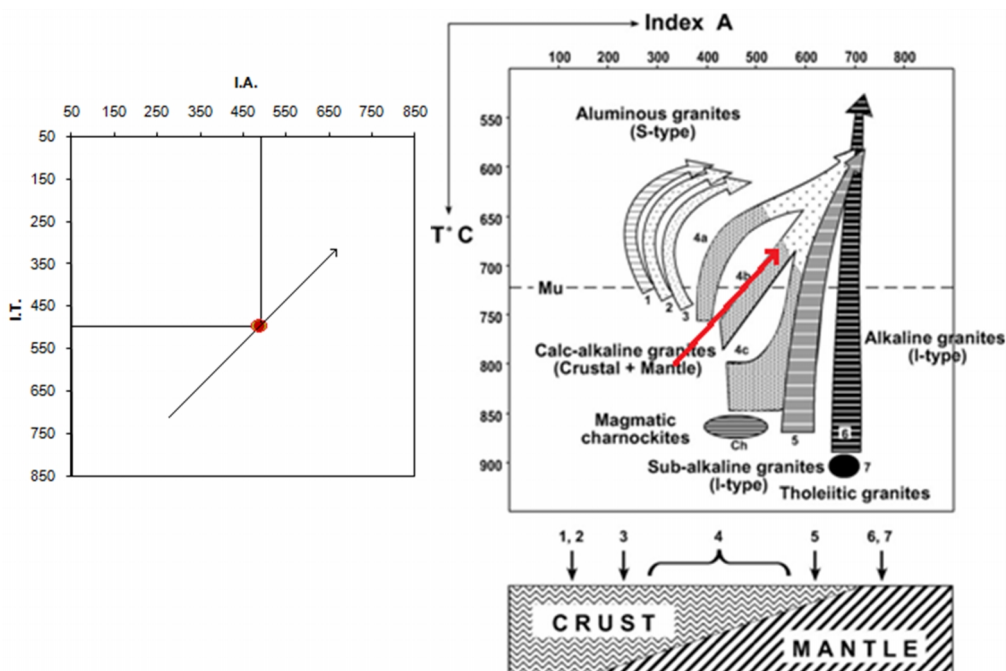


**Figure 18.** The crossing point of I.T and I.A and the value of T.E.T calculated for zircons of the studied area and the position of this trend on Pupin [6] diagram

- b. Absence of congenital zircons and xenocrysts in the selected samples
- c. Even distribution of zircons throughout the whole rock
- d. Perception of negative correlation in Zr vs. Si diagram

With the following evidence, a temperature calculation method based on degree of saturation of zircon can be applied to determine the temperature of crystallization of Mard-abad granite.

- a. The nature of Mard-abad granites is metaluminous type and only one samples falls into peraluminous field
- b. The separation of zircons is carried out in such fashion that no congenital zircon and xenocryst exist
- c. zircon crystals distributed throughout the whole rock (Fig. 20)
- d. Presence of negative correlation in Zr vs. Si diagram

Temperature of zircon crystallization can be determined both through calculation and drawing graph for those samples analyzed with XRF and ICP-AES methods.

**2-1) Temperature calculation method based on degree of zircon saturation**

Watson and Harrison [26] proved the following

equation between zircon solubility, temperature and magma composition:

$$\ln D_{Zr}^{Zircon/melt} = \{-3.80 - [0.85 (M-1)]\} + 12900/T [K]$$

$$T_{Zr} = 12900 / [2.95 + 0.85 M] \ln (496000 / Zr^{melt})$$

In this equation  $\ln D_{Zr}^{Zircon/melt}$  is the ratio of zirconium concentration in zircon mineral to the zirconium concentration in the magma. The number 496000 is the concentration of zirconium in ppm, and T represents the temperature in Kelvin. Also, M is a cation ratio that depends on the solubility ratio of zircon to SiO<sub>2</sub> as well as peraluminous nature of magma, which is calculated using the formula below:

$$M = (Na + K + 2.Ca) / (Al.Si)$$

As shown in Table 2, the crystallization temperature of zircon of Mard-abad granite has been calculated as high as 772.2 to 792 C°. These values are in line with those obtained during studying zircons from morphological standpoint (700 to 800C°).

**2-2) Graph drawing method using the results from analyzed samples**

As shown in Zr vs. SiO<sub>2</sub> diagram by Watson and Harrison [26], Mard-abad granites are placed within

	100	200	300	400	500	600	700	800
550	0	0	0	0	0	0	0	0
600	0	0	0	0	0	0	0	0
650	0	0	0	0	0	0	0	0
700	0	0	0	0	6	8	0	0
750	0	0	0	2	12	0	0	0
800	0	0	2	7	3	0	0	0
850	0	0	0	0	0	0	0	0
900	0	0	0	0	0	0	0	0

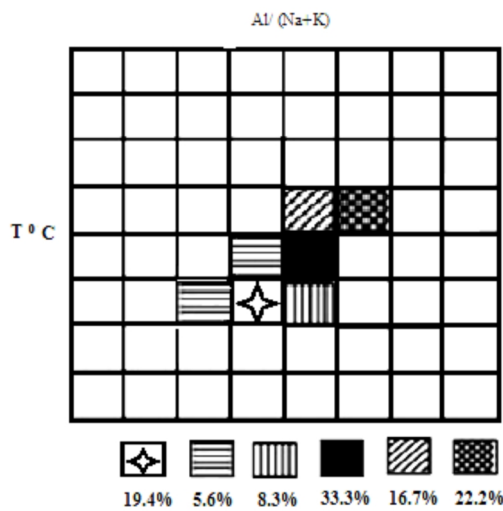


**Figure 19.** Morphological frequency distribution of zircon crystals on the basis of quantity and frequency of occurrence in studied intrusion, and their emplacement within the area of 700 to 800°C on Pupin [6] diagram

temperature areas of 760 to 800 C° (fig. 21), which is similar with the temperature obtained during studying zircons from morphological standpoint (700 to 800C°).

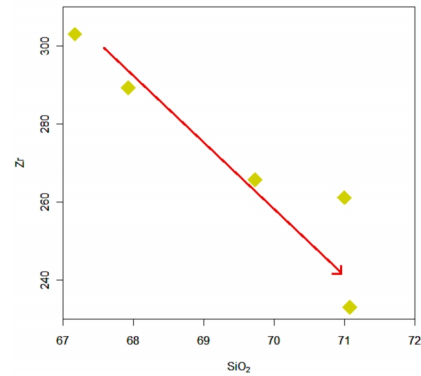


**Figure 20.** Negative correlation between Zr and Si

### Conclusions

The studies on Mard-abad granitic magma, located near Mahdasht, point to metaluminous nature of this magma, and such origin imply to post-collision pull-apart setting behind the arc. Due to the frequency and abundance of granophyric texture and presence of perthite in these granites, it can be concluded that the crystallization is of hypersolvus type and occurred under water vapor pressure of almost 2 kilobars. Considering the chemistry of the whole rock, the temperature at the time of formation of these granites is estimated to be as high as 750 to 800 C°. Morphologically the zircon crystals in the studied area are placed in S10, S14 and S18 areas, and to the lesser amount in S9, S13, S17 and S19 areas of Pupin classification [6]. The shape of zircons of these granites implies to formation of these crystals from hybrid magma, meaning originated from both crust and mantle sources (calc-alkaline and sub-alkaline series). The crystallization temperature of these granites is within 700 to 800 C° based on morphological studies on zircons, 772.2 to 792 C° based on thermometry using zircon saturation, and 760 to 800 C° based on results from XRF and ICP-AES analyses. The result obtained

**Table 2.** The results from analysis of granitic samples and calculation of M, degree of saturation and saturation temperature of zircon for Mard-abad granites

Sample number	SiO2 %	Al2O3 %	CaO %	Na2O %	K2O %	Zr ppm	Zr Saturation		
							M	Zr.sat	TZr.sat.C
G-1	67.17	13.87	1.4	3.65	5.43	303	1.569057	120.7	790.6
E1-90	69.73	12.77	1.16	3.43	5.88	265.7	1.608991	124.9	775.2
E2-90	71	13.57	0.33	3.74	5.56	261.1	1.376217	102.4	792
S-2	67.93	13.6	1.51	3.43	5.31	289.3	1.554823	119.2	787.4
S-8	71.08	12.02	0.55	2.92	6.04	233	1.445631	108.7	775.9

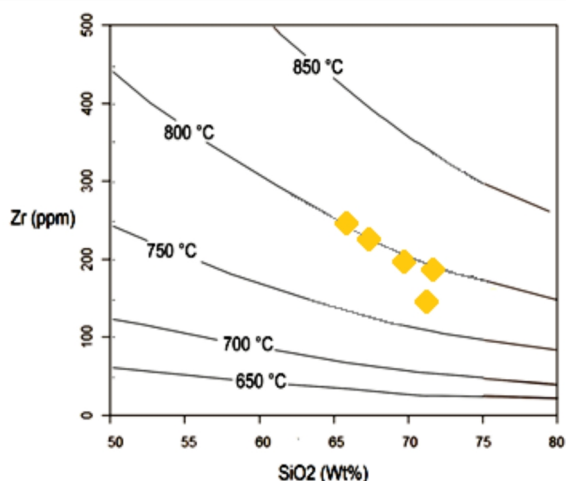


**Figure 21.** Zr vs. SiO<sub>2</sub> diagram by Watson and Harrison [26] for determination of crystallization temperature of Mard-abad granites

from thermometry of zircon crystals is in line with the results from thermometry of texture and chemistry of the whole rock. Lack of hydro-zircon growth is probably due to the zircon crystallization from a relatively dry magma that matches the nature of A type magma.

### References

1. Heaman L., M., Bowins R., Crocket J. The chemical composition of igneous zircon suites: implications for geochemical tracer studies. *Geochim Cosmochim Acta*, **54**:1597-1607 (1990).
2. Hoskin P., W., O., Schaltegger U. The composition of zircon and igneous and metamorphic petrogenesis In: Hanchar J., M., and Hoskin P., W., O. (eds) *Zircon. Reviews in Mineralogy and Geochemistry*, **53**: 27- 62 (2004).
3. Belousova E., A., Griffin W., L., O'Reilly S., Y., Fisher N., J. Igneous zircon: trace element composition as an indicator of source rock type. *Contrib Mineral Petrol*, **143**:602-622 (2002).
4. Corfu F., Hanchar J., M., Hoskin P., W., O., and Kinny P. Atlas of zircon textures. In: Hanchar J. M. & Hoskin P. W. O. (eds). *Zircon. Reviews in Mineralogy and Geochemistry*, **53**: 469-499 (2003).
5. Erdmann S., Wodicka N., Jackson S. E., Corrigan D. Zircon textures and composition: refractory recorders of magmatic volatile evolution? *Contrib Mineral Petrol*, **165**:45-71(2013)
6. Pupin J., P. Zircon and granite petrology. *Contributions to Mineralogy and Petrology*, **73**: 207-220 (1980).
7. Krasnobayev A., A. *Zircon as an Indicator of Geological Processes* (in Russian). Moscow, Nauka, 146 p. (1986).
8. Wang X. Quantitative description of zircon morphology and its dynamics analysis. *Science in China*, **41**: 422-428 (1998).
9. Berezhnaya N., G. Criteria for the genetic typification of zircon from metamagmatic associations of the Aldan Shield. *Doklady Earth Sciences*, **368**: 982-984 (1999).
10. Wang X., and Kienast J., R. Morphology and geochemistry of zircon: a case study on zircon from the microgranitoid enclaves. *Science in China*, **42**: 544-552 (1999).
11. Irvine T., N., Baragar W., K., A. A guide to the chemical classification of the common volcanic rocks, *Can. J. Earth Sci.* **8**: 523-548 (1971).
12. Cox K., G., Bell J., D., Pankhursts R., J. *The interpretation of igneous rocks*, 144p. (1979).
13. Hastie A., R., Kerr A., C., Pearce J., A., and Mitchell S., F. Classification of altered volcanic island arc rocks using immobile trace elements: development of the Th- Co discrimination diagram. *Journal of Petrology* **48**: 2341-2357 (2007).
14. De La Roche H., Leterrier J., Grandclaude P., and Marchal M. A classification of volcanic and plutonic rocks using R1-R2 diagram and major element analyses: its relationships with current nomenclature. *Chemical Geology* **29**: 183-210 (1980).
15. Streckeisen A., Le Maitre R., W. *A Chemical Approximation to the Modal QAPF Classification of the Igneous Rocks*. Neu. Jb. Mineral., Abh, 136, 169.206 (1979).
16. Frost B., R., Barnes C., G., Collins W., J., Arculus S., R., J., Ellis D., J., and Frost C., D. A geochemical classification for granitic rocks. *Journal of Petrology* **42**: 2033-2048 (2001).
17. Shand S., J. *The Eruptive Rocks*, 2nd edn. New York, John Wiley, 444 p (1943).
18. Liégeois J., P., Black R. Alkaline magmatism subsequent to collision in the Pan-African belt of the Adrar des Iforas. In: Fitton J.G., Upton B.G.J. (Eds.). *Alkaline Igneous Rocks*. Geological Society, Blackwell, Oxford, pp. 381-401 (1987).
19. Harris N., B., W., Xu R., Lewis C., L., Hawkeworth C., J., Zhang Y. Isotope geochemistry of the Tibet Geotraverse, Lhasa to Golmud. *Philosophical Transactions of the Royal Society of London* **327**: 263-285 (1988).
20. Pearce J.A., Harris N., B., W., and Tindle A., G. Trace element discrimination diagrams for the tectonic interpretation of granitic rocks. *Journal of petrology*, **25**: 956-983 (1984)

21. Whalen J., B., Currie K., L., Chappell B., W. A-type granites: geochemical characteristics, discrimination and Petrogenesis. *Contrib Mineral Petrol* **95**: 407-419 (1987).
22. Kleman G., J., and Twist D. The compositionally-Zoned sheet like granite pluton of the Bushveld complex. *Jou. Pet.* **30**: 1383- 1414 (1989).
23. Eby G., N. Chemical subdivision of the A-type granitoids, petrogenetic and tectonic implications. *Geology* **20**: 641-644 (1992).
24. Darvishzadeh A. *Geology of Iran* (in Farsi). Neda Publications, Tehran, 901p. (1991).
25. Winkler H. G. F. Petrogenesis of metamorphic rocks. *Springer* (1976).
26. Watson E., B., and Harrison T., M. Zircon saturation revisited: temperature and composition effects in a variety of crustal magma types. *Earth Planet* **64**:295-304 (1983).
27. Janousek V. Saturnin, R. Language script for application of accessory-mineral saturation models in igneous geochemistry. *Geological Carpathica* **57**: 131-142 (2006).